Lattice vibrations in polyacetylene

J. C. Hicks and G. A. Blaisdell
Naval Ocean Systems Center, San Diego, California 92152
(Received 16 July 1984; revised manuscript received 1 October 1984)

The phonon modes for polyacetylene are calculated in the framework of the continuum model. Included are the lattice vibrations in polyacetylene containing the low-lying topological excitations corresponding to a soliton or a polaron, as well as those for the perfectly dimerized chain. Numerical solutions are obtained for the chain containing these topological excitations. The phonon modes for the chain with a soliton are compared to the domain-wall ϕ^4 solutions, and it is shown that the translational or Goldstone mode for the ϕ^4 model is an "exact" solution with $\omega=0$. The chain containing a polaron is found to have four localized vibrational modes, one of which is a translational mode where the frequency is numerically determined to be near zero. Excitation energies including lattice vibrations for a chain containing a soliton or a polaron are also calculated.

I. INTRODUCTION

The soliton model[1-4] for *trans*-polyacetylene, $(CH)_x$, has stimulated a large amount of interest in this material.[5] The charge conjugation symmetry of the models involved[1,3] and the presence of the well-known midgap state in the vicinity of the domain wall leads directly to the unusual charge-spin relations for a soliton in $(CH)_x$. These charge-spin relations and the presence of a midgap state have enabled the soliton model to explain many of the optical,[6,7] magnetic,[8] and electrical[5] properties of this polymer. Moreover, a second type of excitation, a polaron,[9,10] has been recognized as occurring in the same models which predict a soliton or kink solution. For topological reasons a dimerized chain doped with a single charge cannot exhibit a solitonlike excitation. A polaron, which is very similar to a soliton-antisoliton pair, is energetically favored over charge transfer into the conduction band, and is the appropriate excitation for single-charge transfer. The polaron is significant in that with some possible minor modifications it describes excitations relevant to many conjugated polymers which do not exhibit degenerate ground states (e.g., polypyrrole and polyparaphenylene). Consequently, this excitation also merits study.

The object of this paper is to consider the lattice fluctuations of $(CH)_x$ within the framework of the Takayama—Lin-Liu—Maki (TLM) continuum model. The chain will be considered for the three order parameters of the model that are found to satisfy the self-consistent gap equation. These correspond to a dimerized chain with $\Delta(x)=\Delta$, a chain containing a soliton with $\Delta(x)=\Delta\tanh(\Delta x/v_f)$, and a singly-charged chain containing a polaron with $\Delta(x)=\Delta-v_f k_0\{\tanh[k_0(x+x_0)]-\tanh[k_0(x-x_0)]\}$, where $v_f k_0/\Delta=\tanh(2k_0x_0)=1/\sqrt{2}$, and v_f is used to denote the Fermi velocity of the π-electron gas. Single-electron-loop corrections will be included for all three cases. Exact analytical solutions are obtained for the dimerized chain and the translational or "Goldstone"[11] mode for the chain with a soliton. An approximate analytical solution is also obtained for the second bound state on the chain with a soliton. These solutions will be compared with those obtained by Nakahara and Maki[12] in a similar calculation. The remaining phonon modes (as well as the two bound states) for a chain with a kink are obtained numerically and compared to the domain-wall ϕ^4 solutions.[13] The phonon modes for a chain with a polaron will only be obtained numerically and the four resulting localized modes discussed. The excitation energies including lattice vibrations for a chain containing a soliton or a polaron are also calculated.

II. PHONON DISPERSION RELATION

Before considering a chain of polyacetylene with an excitation corresponding to a soliton or a polaron it is worthwhile to consider a perfectly dimerized chain. The excitations to be considered later are localized and will not affect the continuum dispersion relation obtained for a dimerized chain. The continuum model[3] Hamiltonian that allows for lattice vibrations is given by

$$H=\sum_s \int dx\,\psi_s^\dagger(x)\left[-iv_f\frac{\partial}{\partial x}\sigma_3+\Delta(x,t)\sigma_1\right]\psi_s(x)+\frac{1}{2g^2}\int dx[\dot{\Delta}^2(x,t)+\omega_Q^2\Delta^2(x,t)]\,, \tag{2.1}$$

where $\omega_Q^2=4K/M$ and $g=4\alpha\sqrt{a}/M$. K, M, α, and a are the spring constant, effective CH mass, electron-phonon coupling constant, and the lattice spacing of the Su-Schrieffer-Heeger (SSH) model.[1] For a dimerized chain $\Delta(x,t)=\Delta(x)+\delta\Delta(x,t)$ with $\Delta(x)=\Delta$. The phonon Green's function is defined as

$$D(x,x',\tau)=-\langle T_\tau\delta\Delta(x,\tau)\,\delta\Delta(x',0)\rangle\,, \tag{2.2}$$

where T_τ is the imaginary time-temperature ordering operator. Expanding in Matsubara frequencies, $\omega_n=2n\pi/\beta$, the resulting Dyson equation including one-electron-loop corrections is

$$D(x,x',i\omega_n)=d(x,x',i\omega_n) +2d(i\omega_n)\int dy\,\Pi(x,y,i\omega_n)D(y,x',i\omega_n)\ . \tag{2.3}$$

The zeroth-order phonon correlation function represented by $d(x,x',i\omega_n)$ is the appropriate Green's function, ignoring any contribution from the electron-phonon interaction. At this level of approximation only Einstein modes appear at a frequency of ω_Q and

$$d(x,x',i\omega_n)=\frac{g^2\delta(x-x')}{(i\omega_n)^2-\omega_Q^2}=d(i\omega_n)\delta(x-x')\ . \tag{2.4}$$

The kernel in the integral in Eq. (2.3) is due to the polarization of an electron-hole pair and is given by

$$\Pi(x,y)=\frac{1}{\beta}\sum_{\nu_n}\mathrm{Tr}[\sigma_1 g(x,y,i\nu_n)\sigma_1 g(y,x,i\nu_n)]\ , \tag{2.5}$$

where the g's are the appropriate electronic Green's functions. Since the phonon frequencies are substantially less than the electronic gap, 2Δ, the adiabatic approximation has been used and the polarization kernel is taken to be frequency independent. The Matsubara sum in Eq. (2.5) is over odd integers, $\nu_n=(2n+1)\pi/\beta$.

An eigenfunction expansion of $D(x,x',i\omega_n)$ is

$$D(x,x',i\omega_n)=g^2\sum_k\frac{\phi_k(x)\phi_k^*(x')}{(i\omega_n)^2-\omega_k^2}\ . \tag{2.6}$$

Substituting expressions (2.4) and (2.6) into the Dyson equation yields the following integral equation for the phonon eigenfunctions:

$$\omega_k^2\phi_k(x)=\omega_Q^2\phi_k(x)+\lambda\pi v_f\omega_Q^2\int dy\,\Pi(x,y)\phi_k(y)\ , \tag{2.7}$$

where λ is the dimensionless electron-phonon constant, $2g^2/\pi v_f\omega_Q^2$, and is assumed to be 0.378 for this calculation.

It is interesting to note that the effect of the localized excitations of a soliton or polaron on the phonon spectra only appear via the electron-phonon interaction in the kernel, $\Pi(x,y)$. This can be most easily understood by examining the SSH model[1] and including lattice fluctuations. This model has only one spring constant, K, which reflects the harmonic nature of the sigma bond over the range of dimerization ($u_0/a\ll 1$) in polyacetylene. Consequently there is no gap in the dispersion relation for the bare phonons at the edge of the Brillouin zone, reflecting the fact that the bare phonons do not see the dimerization. If the electron-phonon interaction is included then the dispersion relation for the dressed (with electron-loop corrections) phonons exhibits a gap at $k=\pi/2a$.[14] This can be effectively modeled with two spring constants, one for the double bond and one for the single bond. Thus any changes in the dimerization pattern through a local excitation can only be seen through the electron-phonon interaction.

For simplicity the electron Green's functions are expressed in the coordinate representation and the kernel for the dimerized chain is then

$$\Pi_D(x,y)=-\frac{1}{\beta}\sum_{\nu_n}\frac{e^{-2k_n|x-y|}}{v_f^4k_n^2}(v_f^2k_n^2-\Delta^2)\ , \tag{2.8}$$

where $v_f^2k_n^2=\Delta^2-(i\nu_n+\mu)^2$, and for the dimerized chain μ is set equal to 0. Since the kernel only depends on the difference between x and y the eigenfunctions are

$$\phi_k^D(x)=\frac{e^{ikx}}{\sqrt{L}}\ , \tag{2.9}$$

and the resulting coordinate integration in Eq. (2.7) can be performed in a straightforward manner. From self-consistency considerations $(1/\beta)\sum(1/v_f)k_n=1/\pi\lambda$ (see Appendix) and in the notation of Nakahara and Maki,[12]

$$\omega_k^2=\lambda\omega_Q^2\frac{(1+\eta^2)^{1/2}}{\eta}\ln[(1+\eta^2)^{1/2}+\eta] =\omega_0^2\frac{(1+\eta^2)^{1/2}}{\eta}\sinh^{-1}\eta\ , \tag{2.10}$$

where $\omega_0^2=\lambda\omega_Q^2$ and $\eta=v_fk/2\Delta$. Therefore the optical-mode frequency is proportional to the square root of the coupling constant, λ. At first glance this is somewhat surprising. However, due to the nature of the continuum model this dispersion relation should only be considered valid for small η. Since the phonon for small k (or η) is sensitive to the curvature of the adiabatic potential of the electron-hole polarization, and this curvature goes to zero as λ goes to zero, the above result is reasonable.[15] This point is discussed in some detail in this reference.

The zero-point oscillations can easily be determined from these results. Since

$$\langle\delta\Delta^2(x)\rangle=-D(x,x,\tau=0)=-g^2\frac{1}{\beta}\sum_{\omega_n}\frac{|\phi_k^D(x)|^2}{(i\omega_n)^2-\omega_k^2} \tag{2.11}$$

and at room temperature $\beta\omega_0\gg 1$, the sums over ω_n and k can be performed in a straightforward way, yielding

$$\langle\delta\Delta^2(x)\rangle=2.12\omega_0\Delta\ . \tag{2.12}$$

Using the experimentally determined parameters $\omega_0=1460\ \mathrm{cm}^{-1}$ (Ref. 16) and $\Delta=0.7$ eV yields

$$\frac{(\langle\delta\Delta^2(x)\rangle)^{1/2}}{\Delta}=0.74\ . \tag{2.13}$$

These fluctuations are of the same order as the dimerization parameter which is consistent with earlier results.[17] These fluctuations should contribute substantial shape changes to the observed optical-absorption spectra, and it would be of interest to calculate the optical-absorption coefficient including lattice vibrations.

III. SOLITON

As discussed in Sec. II the only change in the Dyson equation is through the electronic Green's functions used in the expression for the kernel, Eq. (2.5). Again this kernel is most easily expressed in the coordinate representation. Using the electronic Green's functions for a soliton,

$\Delta(x)=\Delta\tanh\Delta x/v_f$, obtained earlier,[18] the kernel is expressed as

$$\Pi_s(x,y)=-\frac{1}{\beta}\sum_{\nu_n}\frac{e^{-2k_n|x-y|}}{v_f^4k_n^2}[v_fk_n\mathrm{sgn}(x-y)+\Delta(x)]\times[v_fk_n\mathrm{sgn}(x-y)-\Delta(y)]\ , \tag{3.1}$$

where with no loss in generality μ is again set equal to zero.

Since the continuum model in the absence of a soliton is translationally invariant and the soliton breaks this symmetry, there must be a mode associated with the translation of the soliton domain wall. This translational or Goldstone[11] mode must occur at $\omega_1=0$. For small displacements of the soliton from its original position this mode is proportional to the derivative of $\Delta(x)$, or $\phi_1(x)=a_1\mathrm{sech}^2\Delta x/v_f$. This was recognized in the earlier work by Nakahara and Maki[12] who found an approximate solution of $\phi_1(x)\simeq a_1\mathrm{sech}^{1.95}\Delta x/v_f$ with $\omega_1^2\simeq 0.067\omega_0^2$. Using the kernel shown above and integration techniques discussed in one of the authors' earlier works[18] it is relatively straightforward to show

$$\int\Pi_s(x,y)\mathrm{sech}^2(\Delta y/v_f)dy=-(\lambda\pi v_f)^{-1}\mathrm{sech}^2(\Delta x/v_f)\ . \tag{3.2}$$

Substituting this result into Eq. (2.7) yields $\omega_1^2=0$. The obvious benefit of expressing the kernel in the coordinate representation is the straightforward manner in which the translational mode or Goldstone mode is shown to be an "exact" solution with $\omega_1^2=0$. Since this is also the exact ground-state solution to the domain-wall ϕ^4 model it is tempting to try the other solutions to the ϕ^4 model for the integral equation in (2.7). The ϕ^4 mode corresponding to oscillations of the soliton width is

$$\phi_2(x)=a_2\sinh\Delta x/v_f\mathrm{sech}^2\Delta x/v_f\ .$$

Integrating this function with the kernel in (3.1) yields

$$\int\Pi_s(x,y)\phi_2(y)dy=-\frac{1}{\lambda\pi v_f}\phi_2(x)+\frac{a_2}{\beta}\sum_{\nu_n}\frac{1}{v_fk_n}\left[\Delta(x)-\frac{v_f}{2}\frac{\partial}{\partial x}\right]\int dq\frac{\cos(qx)\mathrm{sech}(\pi v_fq/2\Delta)}{v_f^2q^2+4v_f^2k_n^2}\ . \tag{3.3}$$

Due to the envelope provided by $\mathrm{sech}(\pi v_fq/2\Delta)$, the integral over q above can be approximated as

$$\frac{1}{4v_f^2k_n^2}\int dq\cos(qx)\mathrm{sech}(\pi v_fq/2\Delta)=\frac{\Delta\,\mathrm{sech}(\Delta x/v_f)}{2v_f^3k_n^2}\ . \tag{3.4}$$

Substituting this result into expression (3.3) above yields

$$\int\Pi_s(x,y)\phi_2(y)dy\simeq\frac{1}{\lambda\pi v_f}(-1+3\lambda/4)\phi_2(x)\ . \tag{3.5}$$

The resulting eigenvalue for this domain-wall rocking mode or width oscillation is $\omega_2^2=\frac{3}{4}\lambda\omega_Q^2=\frac{3}{4}\omega_0^2$, which is the same energy as predicted by the ϕ^4 model. However, this solution is not exact but merely a good approximation. The continuum band solutions for the ϕ^4 model are given by

$$\phi_k(x)=A_k\{\Delta^2[3\tanh^2(\Delta x/v_f)-1]-3iv_fk\Delta\tanh(\Delta x/v_f)-v_f^2k^2\}e^{ikx}\ , \tag{3.6a}$$

where

$$kL=(2n+1)\pi+\theta_k\ ,\quad \theta_k=2\tan^{-1}\left[\frac{3v_fk\Delta}{2\Delta^2-v_f^2k^2}\right]\ , \tag{3.6b}$$

$$|A_k|^2=\frac{|a_k|^2}{(4\Delta^2+v_f^2k^2)(\Delta^2+v_f^2k^2)}\ , \tag{3.6c}$$

and

$$|a_k|^2=\left[L-\frac{d\theta_k}{dk}\right]^{-1}\ .$$

These solutions are somewhat unwieldy to consider analytically, but will be compared to numerical solutions for the integral equation (2.7).

Implicit in deriving the kernel in the coordinate representation is that $L\gg v_f/\Delta$. However, to solve the integral equation numerically it is necessary to consider a chain of finite length. Therefore, for the purposes of numerical solutions, the Green's functions, which have been used, were expanded in the appropriate eigenfunctions and sums rather than integrals were performed by taking into account the correct boundary conditions for a chain with a soliton[19] or a polaron.[10] Once the kernel was determined numerically the integral equation (2.7) was first written in the form of an eigenvalue problem as follows:

$$\int\Pi_s(x,y)\phi_k(y)dy=\gamma_k\phi_k(x)\ , \tag{3.7}$$

where $\gamma_k=(\omega_k^2/\omega_Q^2-1)/\lambda\pi v_f$. Following the Nystrom method,[20] the integral in Eq. (3.7) is approximated by a sum

$$\int\Pi_s(x,y)\phi_k(y)dy\cong\sum_j\alpha_j\Pi_s(x,y_j)\phi_k(y_j)\ , \tag{3.8}$$

where α_j are the weights and y_j are the grid coordinates used in an integration scheme. Replacing the integral with the sum and evaluating the integral equation at the points x_i gives a linear algebraic eigenvalue problem. The kernel $\Pi(x,y)$ is real and symmetric so that the eigenfunctions of the integral equation, Eq. (3.7), are real and orthonormal. In order to ensure that the numerical solutions are orthogonal a slight transformation is made. Let $\psi_k(y_j)=(\alpha_j)^{1/2}\phi_k(y_j)$ and $A_{ij}=(\alpha_j)^{1/2}\Pi(x_i,y_j)(\alpha_i)^{1/2}$. Then by multiplying the linear algebraic equation by $(\alpha_i)^{1/2}$ one obtains

$$\sum_j A_{ij}\psi_k(y_j)=\gamma_k\psi_k(x_i)\ . \tag{3.9}$$

A_{ij} is a real, symmetric matrix so eigenvectors corresponding to different eigenvalues are orthonormal, that is $\sum_j \psi_k(y_j)\psi_l(y_j)=\delta_{kl}$. The use of the transformation then ensures that the eigenfunctions are orthonormal with good numerical accuracy since

$$\int \phi_k(y)\phi_l(y)dy \cong \sum_j \alpha_j\phi_k(y_j)\phi_l(y_j)$$
$$=\sum_j \psi_k(y_j)\psi_l(y_j)=\delta_{kl}\ . \tag{3.10}$$

The eigenfunctions $\phi_k(y_j)=\psi_k(y_j)/(\alpha_j)^{1/2}$ were found by solving the linear eigenvalue problem, Eq. (3.9), using a routine from the Internation Mathematical & Statistical Libraries (IMSL).

For the calculations presented here, Simpson's rule with a nonuniform grid spacing was used as the integration scheme. A nonuniform grid was used in order to reduce the number of grid points and hence the size of the matrix A_{ij}. A higher density of grid points was used in the neighborhood where the dimerization pattern changed.

The numerical solutions for these bound-state modes for a chain containing a soliton of length 18ξ, $\xi=v_f/\Delta$, are shown with solid lines in Figs. 1(a) and 1(b). The corresponding solutions to the ϕ^4 model are shown with dashed lines in the same figures. It can be seen that these solutions are in good agreement with one another. The second bound state is a rocking mode in the domain wall, or equivalently a width oscillation. The numerically determined eigenvalue for this mode is $\omega_2^2=0.76\omega_0^2$ which is in excellent agreement with the analytical approximation of $\frac{3}{4}\omega_0^2$.

Three continuum mode solutions are shown in Figs. 2(a), 2(b), and 2(c) with the corresponding solutions of the ϕ^4 model. These are three of the lowest-energy continuum solutions and they do not exhibit as good a fit as the bound-state solutions. In general as the continuum energy increases the numerical solutions show better agreement with the ϕ^4 model solutions which, as can be seen in Eqs. (3.6), become more sinusoidal in nature. The numerically determined eigenvalue for the two lowest-energy continuum modes shown in Figs. 2(a) and 2(b) is $\omega_k=0.99\omega_0$, which is in good agreement with expression (2.10).

A $k=0$ mode is of interest since Levinson's theorem implies that the number of nodes in this mode is equal to the number of bound states. As seen in Fig. 2 and in expression (3.6b) there is no $k=0$ mode for a single soliton. The phonon modes for a soliton-antisoliton (SS) pair do contain a $k=0$ mode which is of the form $3\tanh^2\Delta x/v_f-1$ for both solitons.[21] Consequently this mode has four nodes implying two bound states per soliton.

A more detailed comparison of the extended modes with the ϕ^4 model involves a comparison of the phase shift, θ_k, for these modes with the phase shift of the ϕ^4 model. A numerical determination of the phase shifts for low-lying states in the band is shown in Fig. 3. For

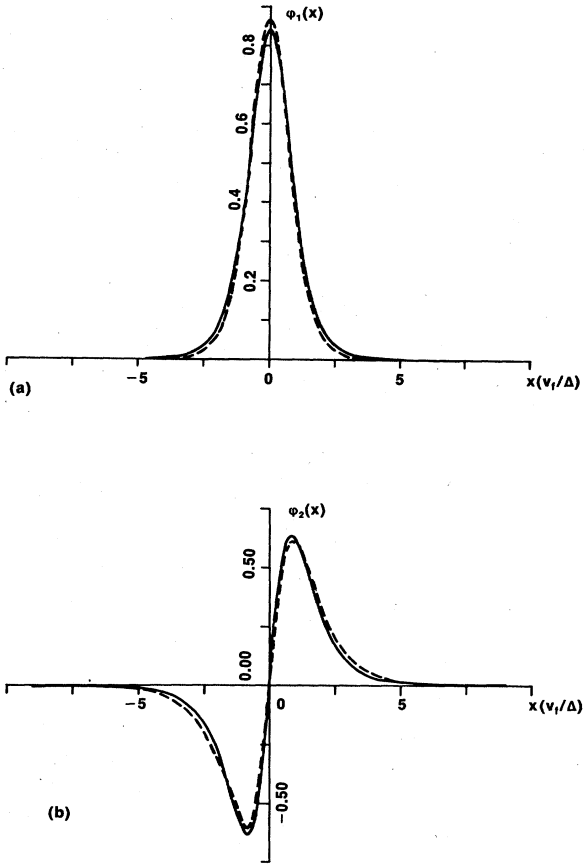

FIG. 1. Bound-state phonon modes for $(CH)_x$ with a soliton, numerical solutions are given by the solid line and the corresponding ϕ^4 solutions are shown with the dashed line.

reasons of numerical accuracy only the phase shifts for the low-lying states were considered reliable. Figure 3 also contains the phase shift of the ϕ^4 model for comparison. With the exception of the phase shift for the lowest-lying state these values are in reasonable agreement with those for the ϕ^4 model. The poor agreement of this first phase shift is thought to be predominantly a result of considering only a single soliton as opposed to a SS pair on the chain.[21] A least-squares fit (excluding the first extended state) of the phase shifts shown in Fig. 3 was performed using the functional form $\theta_k=2\tan^{-1}ak/(b-k^2)$. This resulted in values of $a=3.0$ and $b=3.4$ with a correlation coefficient of better than 0.999. These values are listed in Table I and compared to those for the ϕ^4 model and those calculated by Nakahara and Maki.[12]

The vibrational energy for a polyacetylene chain containing a soliton was calculated assuming a soliton-antisoliton pair. The energy due to zero-point oscillations of a dimerized chain was subtracted from the equivalent value for a chain with a SS pair and the result divided by 2. Assuming the phase shifts for SS to be $kL=2n\pi+2\theta_k$, where $\theta_k=2\tan^{-1}3.0k/(3.4-k^2)$, yields

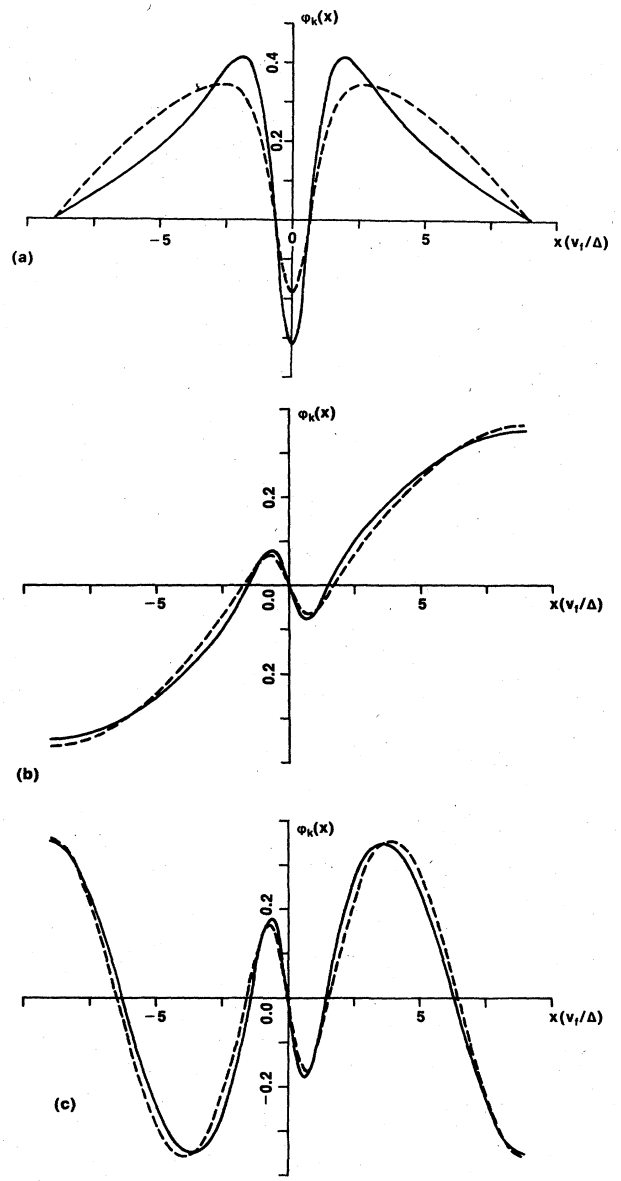

FIG. 2. Continuum phonon modes for $(CH)_x$ with a soliton, numerical solutions are given by the solid line and the corresponding ϕ^4 solutions are shown with the dashed line.

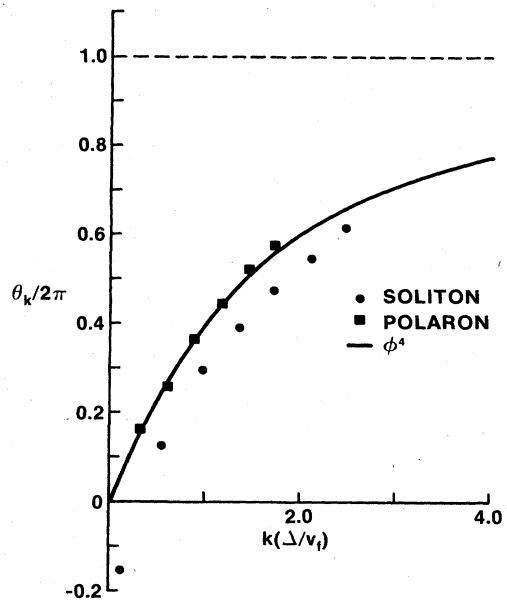

FIG. 3. Phase shifts of the low-lying extended modes for $(CH)_x$ with a soliton, ●, and one-half of the phase shifts for $(CH)_x$ with a polaron, ■. The solid line is the phase shift for the ϕ^4 model.

$$\tfrac{1}{2}\sum_k \omega_k - \tfrac{1}{2}\sum_q \omega_q = -1.21\omega_0 \,. \tag{3.11a}$$

Consequently the excitation energy per soliton is

$$E(\Delta(x))-E(\Delta)=\frac{2\Delta}{\pi}-0.61\omega_0=0.75\frac{2\Delta}{\pi} \,. \tag{3.11b}$$

This excitation energy is virtually identical to that obtained by Nakahara and Maki.[12] To some extent this is coincidental since the energy they obtain for the second bound state is different from ours, they modulate ω_k with a $\cos ka/2$ term, and their phase shifts are also somewhat different. It should also be noted that just as in the case for the electronic excitations it is important to consider a soliton-antisoliton pair and then divide the result by 2. This is because there is no $k=0$ mode in the continuum band for a single soliton. However, there is a $k=0$ mode for the dimerized chain and the chain containing a soliton-antisoliton pair. These excitation energies are substantial, $\sim\frac{1}{4}E_s$, and will be compared to those for a polaron in the next section.

IV. POLARON

Once again, the only change in the integral equation (2.7) is through the electronic Green's functions used in the kernel. With the gap parameter for the polaron,

$$\Delta(x)=\Delta-v_f k_0[\tanh k_0(x+x_0)-\tanh k_0(x-x_0)]$$

with $\sinh 2k_0x_0=1$ and $v_fk_0/\Delta=1/\sqrt{2}$, the kernel in the coordinate representation is

$$\Pi_p(x,y)=-\frac{1}{\beta}\sum_{\nu_n}\frac{e^{-2k_n|x-y|}}{v_f^4k_n^2}\frac{v_f^2k_n^2-\Delta^2}{v_f^2k_n^2-v_f^2k_0^2}$$
$$\times\{v_fk_n\mathrm{sgn}(x-y)+v_fk_0\tanh[k_0(x+x_0)]\}\{v_fk_n\mathrm{sgn}(x-y)+v_fk_0\tanh[k_0(x-x_0)]\}$$
$$\times\{v_fk_n\mathrm{sgn}(x-y)-v_fk_0\tanh[k_0(y+x_0)]\}\{v_fk_n\mathrm{sgn}(x-y)-v_fk_0\tanh[k_0(y-x_0)]\} \,. \tag{4.1}$$

TABLE I. Coefficients for the phase shifts, $\theta_k = 2\tan^{-1}[ak/(b-k^2)]$. The polaron phase shifts are given by $\theta_k = 4\tan^{-1}[ak/(b-k^2)]$.

Model	a	b
soliton (current)	3	3.4
soliton (Ref. 12)	2.1	1.8
ϕ^4	3	2
polaron (current)	2.7	1.9

For this problem it is necessary to specify the chemical potential consistent with a single excess charge in one of the bound states of the polaron. An n-type polaron was chosen with $\mu=\omega_0=(\Delta^2-v_f^2k_0^2)^{1/2}$. The polaron also breaks the translational symmetry and should have a Goldstone mode. The eigenfunction for this Goldstone mode should be

$$\phi_1(x)=a_1\left[\frac{1}{\cosh^2[k_0(x+x_0)]}-\frac{1}{\cosh^2[k_0(x-x_0)]}\right], \tag{4.2}$$

with $\omega_1^2=0$. To test this solution analytically, as was done with the soliton, is extremely tedious and hence not attempted. However, this function is plotted versus the numerical solution in Fig. 4(a). Due to the excellent fit seen in this figure and the obtained eigenvalue of $\omega_1^2=0.048\omega_0^2$, it is felt by the authors that this is in fact an exact solution with $\omega_1^2=0$. There are three other bound-state vibrational modes associated with the polaron which are also shown in Fig. 4. The first true vibrational state has an eigenvalue of $\omega_2^2=0.46\omega_0^2$ and is approximated by a symmetric combination of the translational modes for a soliton-antisoliton pair. This normal mode is approximately a breathing mode of the polaron order parameter. The next excited state has an eigenvalue of $\omega_3^2=0.75\omega_0^2$ and is shown in Fig. 4(c). This mode is approximately an antisymmetric combination of the SS rocking modes. Since a symmetric combination of the SS translational modes and an antisymmetric combination of the rocking modes result in a somewhat similar distortion of the polaron order parameter, there is some mixing in these combinations for the second and third bound phonon states. The fourth bound-state phonon mode has an eigenvalue of $\omega_4^2=0.91\omega_0^2$ and is shown in Fig. 4(d). This mode is almost a pure symmetric combination of the SS rocking modes.

The continuum states are shown in Fig. 5. Figure 5(a) is the $k=0$ mode with $\omega_k=0.99\omega_0$. This mode is extremely similar to the $k=0$ mode for a closely-lying SS pair. Again consistent with Levinson's theorem the number of nodes (four) for the $k=0$ mode is equal to the number of bound states. The rest of the continuum states also are similar to the equivalent states for a closely-lying SS pair. An example is shown in Fig. 5(b).

Again using a chain of length 26ξ, numerical calculations of the phase shifts are shown in Fig. 3. For comparison with ϕ^4 and those of the soliton the values shown in

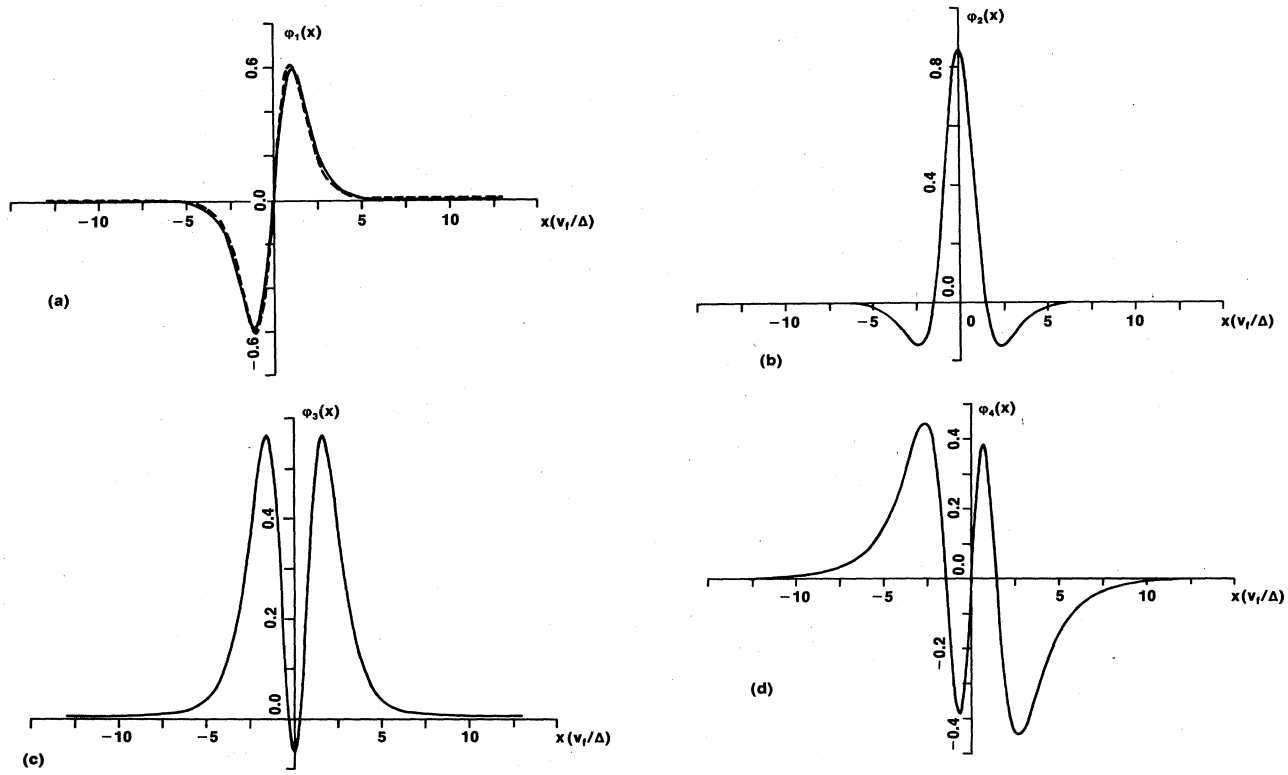

FIG. 4. Bound-state phonon modes for $(CH)_x$ with a polaron, numerical solutions are given by the solid line and the derivative of the order parameter (Goldstone mode) is shown with a dashed line in (a).

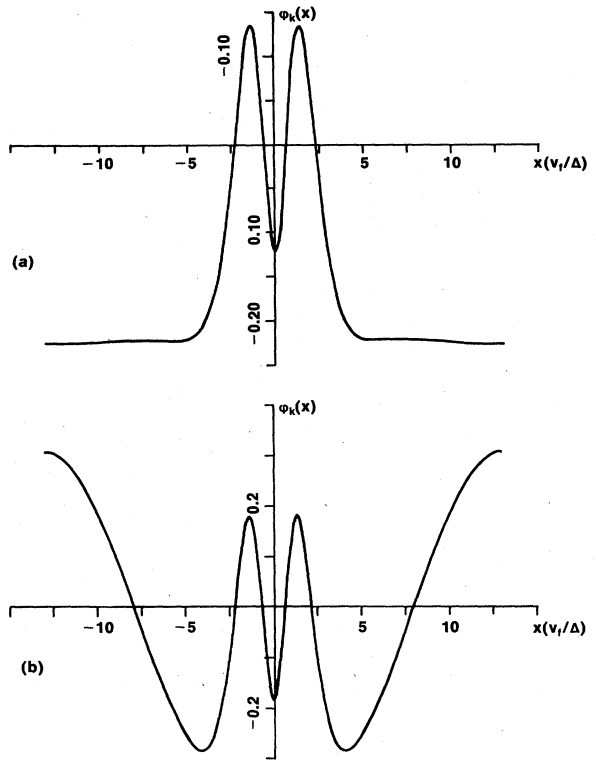

FIG. 5. Numerical solutions for the continuum phonon modes in $(CH)_x$ with a polaron. The eigenstate shown in (a) is the $k=0$ mode.

Fig. 3 are one-half of the actual phase shift. A least-squares fit was again performed with the functional form $\theta_k = 4\tan^{-1}ak/(b-k^2)$. This resulted in values of $a=2.7$ and $b=1.9$ with a correlation coefficient in excess of 0.999. These values are also listed in Table I.

The vibrational energy for a chain with a polaron was calculated with this phase shift and

$$\tfrac{1}{2}\sum_k \omega_k - \tfrac{1}{2}\sum_q \omega_q = -0.88\omega_0 \,. \tag{4.3}$$

This result, as expected, is approximately midway between the decrease in vibrational energy for a single-soliton and a soliton-antisoliton pair. The excitation energy for a polaron is then

$$E(\Delta(x))-E(\Delta)=\frac{2\sqrt{2}\Delta}{\pi}-0.88\omega_0=0.75\left[\frac{2\sqrt{2}\Delta}{\pi}\right]. \tag{4.4}$$

It is interesting that the change in excitation energy is almost in exact proportion to the electronic excitation energy. The energetics for a doubly charged chain still favor an SS pair over a doubly charged polaron (bipolaron) or two polarons. Thus the energy required to create an SS pair or a polaron is substantially reduced, but the relative effects are still consistent with those for a rigid lattice.

V. CONCLUSION

The phonon modes for polyacetylene have been calculated using the continuum version of the SSH model including lattice fluctuations. The dispersion relation for the optical band is in agreement with that of an earlier calculation by Nakahara and Maki.[12] Analytical and numerical solutions were obtained for the localized modes that occur in the presence of a soliton. The analytical solutions are essentially those of the ϕ^4 model and are in excellent agreement, both eigenfunctions and eigenvalues, with the numerical solution. Only numerical solutions were obtained for the normal modes in the continuum band and these solutions with their phase shifts show good agreement with the continuum eigenfunctions of the ϕ^4 model.

A one-component model is not general enough to make any realistic predictions of the Raman and infrared modes observed in $(CH)_x$; however, some of the experimentally observed Raman modes may be attributed to the rocking modes. From calculations involving the discrete lattice[22] and recent experimental observation of resonant Raman scattering,[16] the optical band edge, ω_0, for $(CH)_x$ is assumed to be 1460 cm^{-1}. From the numerical solution for the Raman-active localized mode, $\omega_2=\sqrt{0.76}\omega_0$ and $\omega_2=1273$ cm^{-1}, which is in good agreement with the observed value of 1291 cm^{-1}.[16] For $(CD)_x$ the agreement is equally as good. Assuming a band edge of 1355 cm^{-1} (Ref. 16) for $(CD)_x$, then $\omega_2=1181$ cm^{-1} as compared to the measured value of 1197 cm^{-1}.[16] However, these experimentally observed frequencies may be the band edge of different modes.[22] Since the problem considered in this work does not include any pinning, the translational, or Goldstone, mode occurs at $\omega_1=0$. Inclusion of a pinning parameter could adjust this mode up to the accepted value for $(CH)_x$ of 900 cm^{-1}.[23] In fact a normal mode analysis within the framework of the continuum model does give good agreement with all of the Raman-active and infrared-active modes of $(CH)_x$ and $(CD)_x$.[24] This calculation also yields some very interesting product rules involving the ratios of the infrared and Raman-active modes; however, this calculation does require a six-parameter fit.[24]

The phonon modes for polyacetylene with a singly-charged polaron were also calculated within the framework of the continuum model. A translational mode was also found at $\omega_1=0$, and as expected, is given by the derivative of the order parameter. However, a *trans*-polyacetylene sample must be lightly doped to observe these infrared-active modes as heavy doping gives rise to SS pairs. The frequency for the infrared-active pinned translational mode should be given by the frequency for the pinned mode for a soliton multiplied by the square root of the ratio of the effective masses of the soliton and the polaron. Due to the small effective mass of the polaron,[10] this frequency is above the band edge, making it difficult to observe.

There is one very interesting point to be made concerning the infrared-active localized modes associated with a polaron. Simply, there are two of them, the Goldstone mode and the highest-energy localized mode. This is in

contrast to the normal mode analysis mentioned above[24] in which there is a one-to-one correspondence between infrared-active modes and the electron-phonon-coupled Raman bands. In the normal mode analysis the difference between any configuration is contained in an effective-mass parameter, but does not affect the one-to-one correspondence between the Raman modes and the infrared modes. Therefore this model should be reexamined at least for configurations other than a single soliton.

Finally, due to similar symmetries the phonon modes for the ϕ^4 model are in good agreement with those for polyacetylene with a soliton. Further analytical calculations within the framework of the continuum model, which involve the inclusion of lattice fluctuations, would be justified in using the ϕ^4 solutions as a good approximation to the correct phonon modes.

ACKNOWLEDGMENTS

The authors wish to thank A. L. Wasserman and E. J. Mele for helpful discussions. This work was supported by the Independent Research Program at the Naval Ocean Systems Center.

APPENDIX: SELF-CONSISTENCY

The self-consistency relation is given by

$$\sum_s \psi_s^\dagger(x)\sigma_1\psi_s(x)+\frac{\omega_Q^2}{g^2}\Delta(x)=0 . \tag{A1}$$

The expectation value of this relation at finite temperature is

$$\sigma_1 G(x,x,\tau=0)=-\frac{\omega_Q^2}{2g^2}\Delta(x) . \tag{A2}$$

After expanding in Matsubara frequencies,

$$\frac{1}{\beta}\sum_{\nu_n}\sigma_1 G(x,x,i\nu_n)=-\frac{\omega_Q^2}{2g^2}\Delta(x) . \tag{A3}$$

Since the resulting cutoff in the Matsubara sum is independent of the order parameter (for the gap parameters that satisfy self-consistency) the simple case of a dimerized chain, $\Delta(x)=\Delta$, will be considered. The required Green's functions can be deduced from one of the author's earlier works,[18] and for the chemical potential μ set equal to zero, Eq. (A3) becomes

$$\frac{1}{\beta}\sum_{\nu_n}\frac{1}{v_f^2 k_n}=\frac{\omega_Q^2}{2g^2} . \tag{A4}$$

In terms of the dimensionless electron-phonon coupling constant

$$\frac{1}{\beta}\sum_{\nu_n}\frac{1}{v_f k_n}=\frac{\omega_Q^2 v_f}{2g^2}=\frac{1}{\pi\lambda} . \tag{A5}$$

[1]W. P. Su, J. R. Schrieffer, and A. J. Heeger, Phys. Rev. Lett. **42**, 1698 (1979); Phys. Rev. B **22**, 2099 (1980), **28**, 1138(E) (1982).
[2]M. J. Rice, Phys. Lett. **71A**, 152 (1979).
[3]H. Takayama, Y. R. Lin-Liu, and K. Maki, Phys. Rev. B **21**, 2388 (1980).
[4]A. Brazovskii, Zh. Eksp. Teor. Fiz. **78**, 677 (1980) [Sov. Phys.—JETP **51**, 342 (1980)].
[5]See, for example, the review article by S. Etemad, A. J. Heeger, and A. G. MacDiarmid, Annu. Rev. Phys. Chem. **33**, 443 (1982), and the references therein.
[6]N. Suzuki, M. Ozaki, S. Etemad, A. J. Heeger, and A. G. MacDiarmid, Phys. Rev. Lett. **45**, 1209 (1980).
[7]A. Feldblum, J. H. Kaufman, S. Etemad, A. J. Heeger, T.-C. Chung, and A. G. MacDiarmid, Phys. Rev. B **26**, 815 (1982).
[8]S. Ikehata, J. Kaufer, T. Woerner, A. Pron, M. A. Druy, A. Sivak, A. J. Heeger, and A. G. MacDiarmid, Phys. Rev. Lett. **45**, 1123 (1980).
[9]D. K. Campbell and A. R. Bishop, Phys. Rev. B **24**, 4859 (1981).
[10]D. K. Campbell, A. R. Bishop, and K. Fesser, Phys. Rev. B **26**, 6862 (1982).
[11]J. Goldstone, Nuovo Cimento **19**, 154 (1961).
[12]M. Nakahara and K. Maki, Phys. Rev. B **25**, 7789 (1982).
[13]Y. Wada and J. R. Schrieffer, Phys. Rev. B **18**, 3897 (1978).
[14]H. J. Schultz, Phys. Rev. B **18**, 5756 (1978).
[15]S. Kivelson (unpublished)
[16]Z. Vardeny, E. Ehrenfreund, O. Brafman, and B. Horovitz, Phys. Rev. Lett. **51**, 2326 (1983).
[17]W. P. Su, Solid State Commun. **42**, 497 (1982).
[18]J. C. Hicks and A. L. Wasserman, Phys. Rev. B **29**, 808 (1984).
[19]S. Kivelson, T. K. Lee, Y. R. Lin-Liu, I. Peessbel, and Lu Yu, Phys. Rev. B **25**, 4173 (1982).
[20]See, for example, K. E. Atkinson, *A Survey of Numerical Methods for the Solution of Fredholm Integral Equations of the Second Kind* (Soc. Indus.-Appl. Math., 1976).
[21]J. C. Hicks and G. A. Blaisdell (unpublished).
[22]E. J. Mele and M. J. Rice, Solid State Commun. **34**, 339 (1980).
[23]C. R. Fincher, Jr., M. Ozaki, A. J. Heeger, and A. G. MacDiarmid, Phys. Rev. B **19**, 4140 (1979).
[24]B. Horovitz, Solid State Commun. **41**, 729 (1982).